

---

# PET Scanning with Hydroxyephedrine: An Approach to the Localization of Pheochromocytoma

Barry L. Shulkin, Donald M. Wieland, Markus Schwaiger, Norman W. Thompson, Isaac R. Francis, Michael S. Haka, Karen C. Rosenspire, Brahm Shapiro, James C. Sisson, and David E. Kuhl

*Departments of Internal Medicine, Division of Nuclear Medicine, Radiology and Surgery, University of Michigan Medical Center, Ann Arbor, Michigan*

---

Pheochromocytomas are potentially curable causes of hypertension. These tumors are currently located by functional imaging with *meta*-iodobenzylguanidine (MIBG), usually labeled with <sup>131</sup>I, or anatomic imaging (computed tomography, magnetic resonance). Hydroxyephedrine (HED) is a newly developed radiotracer that concentrates in adrenergic nerve terminals. When HED is labeled with <sup>11</sup>C, its distribution can be mapped *in vivo* using PET. The purposes of this investigation were to characterize the uptake of <sup>11</sup>C-HED in pheochromocytoma and to determine the feasibility and advantages of utilizing this compound as a tumor imaging agent. Ten patients with known or suspected pheochromocytoma were studied. Each patient underwent PET scanning with <sup>11</sup>C-HED and conventional scintigraphy with MIBG. Pheochromocytomas were localized by PET scanning in 9 of the 10 patients. Image quality was excellent and superior to that obtained from planar and tomographic MIBG studies. The uptake of <sup>11</sup>C-HED into pheochromocytomas was rapid; tumors were evident within 5 min following intravenous injection. All lesions within the field of view that were identified by MIBG scintigraphy were readily apparent. PET scanning with <sup>11</sup>C-HED localizes pheochromocytoma using a specifically designed radiotracer and advanced imaging technology. The method has promise for locating the more elusive tumors.

**J Nucl Med 1992; 33:1125-1131**

---

**P**heochromocytoma is a rare but important cause of hypertension (1,2). These catecholamine-producing tumors may be lethal if untreated; many are still discovered only at autopsy (3). However, the tumors are usually curable by surgical resection. The diagnosis is sought through a combination of history, physical examination and laboratory determinations of plasma and urinary catecholamines and their metabolites. Once the diagnosis is established, localization becomes critical to patient man-

agement and directs the approach to surgical removal. Although most pheochromocytomas are located within the adrenal glands, they may be found in regions from the neck to the pelvis. Precise localization will spare patients whose disease is either extra-adrenal or metastatic unnecessary exploratory surgery.

Currently, the principal methods of localization are scintigraphy using MIBG (*meta*-iodobenzylguanidine) and computed tomography (CT). CT provides excellent images of the adrenal gland. Its sensitivity for the detection of pheochromocytoma is high, since approximately 90% lie within the adrenal glands (4). However, CT does not differentiate pheochromocytoma from other causes of adrenal enlargement, such as cortical adenomas, carcinomas and metastatic disease, and it is considerably less sensitive for the detection of extra-adrenal involvement (5).

Magnetic resonance imaging (MRI) also provides images with excellent anatomic detail but suffers many of the same limitations as CT (5,6). Neither CT nor MR defines the functional nature of adrenal disorders. Searches for pheochromocytomas by arteriography and venous sampling are invasive and are now rarely necessary.

The detection of pheochromocytoma was advanced by the development and introduction of MIBG, the first radiotracer used to image elements of the sympathetic nervous system and related tumors in man (7, 8). Scintigraphy with MIBG enables a noninvasive screening of the entire body for deposits of pheochromocytoma. The method is both sensitive (88%) and specific (99%), and it is especially helpful in identifying pheochromocytomas outside the adrenal gland as well as recurrent and metastatic disease (9-11). However, the imaging characteristics of the <sup>131</sup>I radionuclide are not ideal: the gamma photons are highly energetic, and only 20% are detected by modern cameras; a substantial amount of radiation is imparted as beta particles, which are not detected by gamma cameras; and the physical half-life (8.1 days) is long, all of which severely restrict the administered activity. Since MIBG is relatively nonpolar, nonspecific binding is high early after injection, and optimal tumor-to-nontumor ratios are not achieved until several days after injection

---

Received Nov. 19, 1991; revision accepted Jan. 31, 1992.  
For reprints contact: Barry L. Shulkin, MD, University of Michigan Medical Center, Pediatric Nuclear Medicine, MCHC F3341, Ann Arbor, MI 48109-0229.

(9–11). MIBG labeled with  $^{123}\text{I}$  overcomes some of the disadvantages of [ $^{131}\text{I}$ ]MIBG, but a number of shortcomings remain (12).

Carbon-11-hydroxyephedrine (HED) is a radiotracer developed to image the sympathetic nervous system (13). HED is more polar than MIBG and bears closer structural similarity to norepinephrine. Biodistribution studies in experimental animals and man have shown selective uptake in organs with rich sympathetic innervation, including the heart and adrenal medulla (13,14). When HED is labeled with  $^{11}\text{C}$ , its distribution can be mapped in vivo with positron emission tomography (PET). PET offers improved imaging technology over conventional single-photon techniques: the use of agents labeled with short-lived radionuclides allows administration of larger tracer doses, resulting in images of higher count density and superior quality; and the three-dimensional reconstruction more precisely depicts the spatial relationship of areas of uptake to the location of nearby organs. We hypothesized that  $^{11}\text{C}$ -HED would rapidly concentrate in pheochromocytomas and, that, using PET to detect focal accumulations of HED, both the anatomic site and the functional nature of adrenergic tumors would be portrayed in high quality images within minutes after injection. The purposes of the present investigation were to evaluate the feasibility of PET scanning with  $^{11}\text{C}$ -HED for localizing pheochromocytomas and to compare its advantages to those of other techniques.

## METHODS

### Patients

Ten subjects (8 male, 2 female), aged 23–72, with known or suspected pheochromocytoma participated in this study. Patients were referred from the Nuclear Imaging and Endocrine Surgery clinics of the University of Michigan. Clinical and biochemical

characteristics are described in detail in Table 1. Patients 2–6, 8 and 10 had previously undergone resection of pheochromocytoma and had recurrent disease.

Pheochromocytomas were subsequently removed from Patients 1, 7 and 9. Antihypertensive medications were continued, and none of the subjects were receiving treatments known to interfere with transport of catecholamines into sympathetic neuronal terminals (15).

Imaging studies consisted of PET scanning with  $^{11}\text{C}$ -HED, scintigraphy with MIBG and anatomic evaluation with CT or MRI as follows.

### PET

**Radiochemistry.** The synthesis of  $^{11}\text{C}$ -HED has been described in detail elsewhere (13). Briefly,  $^{11}\text{C}$ -HED was produced by direct N-methylation of metaraminol with  $^{11}\text{C}$ -methyl iodide in DMF/DMSO and purified by reverse-phase HPLC in an isotonic aqueous buffered system. The specific activity was  $>1000$  Ci/mmol at the end of synthesis, and radiochemical and chemical purities were 95%–98%.

**Data Acquisition.** Patients were positioned in a Siemens/CTI 931 whole-body PET scanner using correlative MIBG, CT and MR images for tumor localization. This device generates 15 cross-sectional images (8 direct, 7 cross planes) and has an intrinsic resolution of 5.2 mm FWHM and a slice thickness of 6.5–8.0 mm. A 20-min transmission scan of the region of the tumor was acquired for attenuation correction using a retractable  $^{68}\text{Ge}$  source. Patients received an intravenous bolus injection of 20 mCi  $^{11}\text{C}$ -HED. Imaging of the tumors was begun immediately after tracer administration and continued for 20 min. One 10-min view of an additional region believed to contain tumor was subsequently obtained.

**Data Analysis.** The data were reconstructed into transverse cross-sectional images using filtered backprojection and a Hanning filter with a cutoff frequency of 0.35 per pixel. In the later images, regions of interest (ROIs) were placed over the tumor, adjacent background, and identifiable noninvolved organs, including the liver and kidney when within the field of view. These regions were copied to all time frames and time-activity curves

TABLE 1  
Clinical and Biochemical Characteristics

Patient no.	Year of Age diagnosis	Sites of tumor	Plasma NE	Plasma E	Plasma D	Urine NE	Urine E	Urine NM	Urine MN	Urine VMA	
1	23	1990	Right and left adrenal	2317	112	<30	332	2	560	39	5.3
2	49	1980	Axial skeleton	4359	<30	501	320	2.5	2801	62	25.7
3	50	1978	Mediastinum, abdomen	219	<30	62	28	1	769	34	17.8
4	35	1964	Lungs, axial skeleton, abdomen	5950	24	109	1236	10	5746	139	5
5	43	1963	Skull, rib, sternum	4149	63	<30	283	8	1655	37	5.9
6	42	1978	Para-aortic	2545	63	<30	194	2	2179	63	3.7
7	34	1989	Mid-abdomen	778	<30	3396	62	18	497	88	11.9
8	60	1959	Skull, spine, chest, abdomen, pelvis	1071	79	<30	83	13	3521	801	8.4
9	72	1990	Left adrenal	711	213	<30	46	19	585	119	4.1
10	43	1974	Para-aortic	879	243	<30	145	65	4635	2820	14.9
			Normal values	0–500	0–100	0–100	0–100	0–20	50–800	0–300	0–7.0
				pg/ml	pg/ml	pg/ml	$\mu\text{g}/24$ hr	$\mu\text{g}/24$ hr	$\mu\text{g}/24$ hr	$\mu\text{g}/24$ hr	mg/24 hr

NE = norepinephrine, E = epinephrine, D = dopamine, NM = normetanephrine, MN = metanephrine and VMA = vanillymandelic acid.

were generated. Tumor-to-nontumor ratios of radioactivity were calculated. Results are expressed as mean  $\pm$  s.e.m.

### MIBG Scintigraphy

All patients underwent MIBG scintigraphy within 2 wk of the PET examination, with the exception of Patient 2, whose most recent study was 6 mo earlier. Patients 1, 3 and 5 received [ $^{131}\text{I}$ ]MIBG, Patients 4 and 7–10, [ $^{123}\text{I}$ ]MIBG and Patients 2 and 6, both. Iodine-123-MIBG was preferred when available.

**Iodine-131-MIBG.** Scintigraphy was performed as previously described (9). In brief, overlapping anterior and posterior images from the top of the head to the knees were acquired for 100,000 counts or 20 min, whichever came first, at 24, 48 and 72 hr following the administration of 0.5 mCi [ $^{131}\text{I}$ ]MIBG. Data were acquired on a large field of view gamma camera with a high-energy collimator interfaced to a Siemens Microdelta computer. ROIs were drawn over areas of abnormal uptake and surrounding background, and the geometric means calculated for tumor-to-nontumor ratios.

**Iodine-123-MIBG.** Following the intravenous administration of 10 mCi [ $^{123}\text{I}$ ]MIBG, both planar and tomographic images were obtained (12) as follows.

1. Planar. Immediately following injection, 10-min spot views of the tumor were acquired. Anterior and posterior views of the entire body were next acquired for 10 min at 2 and 24 hr, and 15-min images at 48 hr. A dual-headed Siemens gamma camera with a low-energy collimator interfaced to a Microdelta computer was utilized. ROIs were drawn as described for [ $^{131}\text{I}$ ]MIBG studies.
2. SPECT. Tomography was performed at 2 and 24 hr using a GE 400 AT camera with a low-energy collimator. The camera was rotated through 360° with 64 stops of 20 sec. Data were reconstructed using filtered backprojection, a Butterworth filter and a cutoff frequency of 0.2–0.5. From the transverse reconstructions, ROIs were defined over the tumor and adjacent background, similar to the PET examination.

### CT

Scans were obtained in Patients 1, 3, 4 and 6–9 using a GE CT/T 9800 scanner (General Electric Medical Systems Group, Milwaukee, WI) with contiguous 10-mm sections.

### MRI

Imaging was performed in Patient 5 with a Diasonics MT/S superconducting magnet (Diasonics, Milpitas, CA). Spin-echo images were obtained at repetition times (TR) of 500–2000 msec with echo times (TE) of 30–60 msec to provide T<sub>1</sub>- and T<sub>2</sub>-weighted images.

### Plasma Catecholamines

These were determined by HPLC immediately prior to and 30 min following administration of  $^{11}\text{C}$ -HED. Twenty-four hour urinary catecholamines and their metabolites were measured the day of the PET study. Blood pressure was monitored throughout the PET procedure.

### RESULTS

PET scanning with  $^{11}\text{C}$ -HED rapidly and clearly detected foci of pheochromocytoma in 9 of 10 patients with pheochromocytoma. The study of Patient 1 is presented in Figure 1. This 23-yr-old woman experienced headaches, palpitations, anxiety, sweating and hypertension at 26 wk gestation. After an uneventful delivery, she underwent CT scanning of the abdomen, which showed enlargement of both adrenal glands, and was referred to this institution for further diagnostic evaluation and therapy. Figure 1 (left) is a transverse section through the upper abdomen obtained only 10 min following injection of  $^{11}\text{C}$ -HED. Intense uptake is noted in the region of the right adrenal, and less intense uptake is present on the left (arrows). These areas correspond to the enlarged adrenal glands evident on CT scanning (Fig. 1, center). The adrenal glands were removed surgically and contained pheochromocytoma-

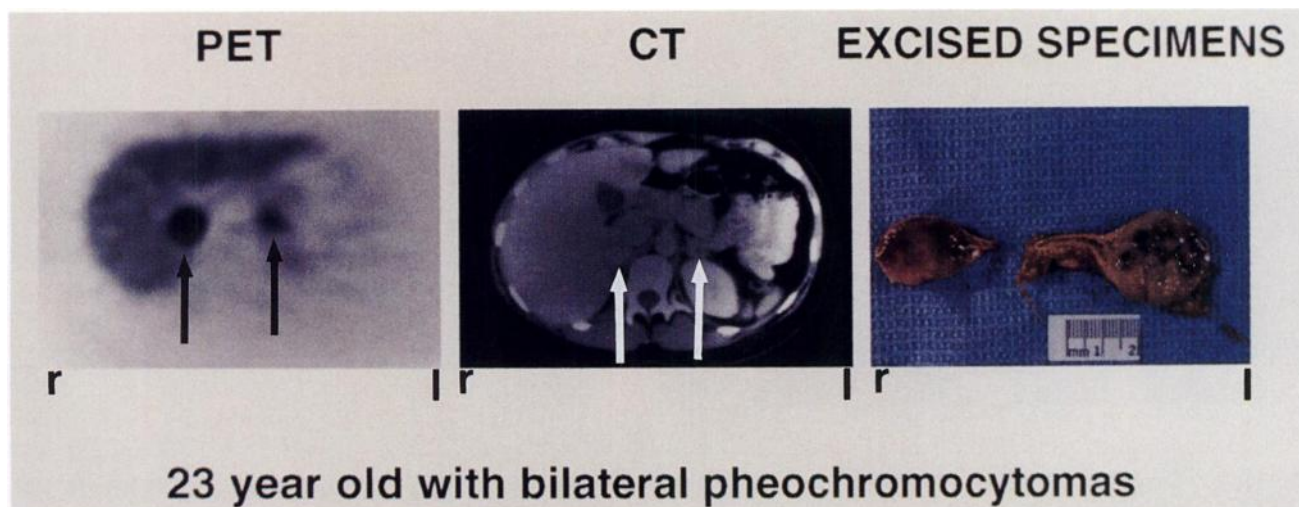


**FIGURE 1.** Patient 1. (Left) HED PET scan of the mid-abdomen acquired 10 min following injection. There is intense uptake within the right adrenal mass and moderately increased uptake in the left adrenal mass (arrows). (Center) CT scan shows bilateral adrenal enlargement (arrows) with partial necrosis of the left gland. (Right) Intact surgical specimen of the adrenals. The left adrenal is considerably larger than the right but much of the tissue is necrotic. These masses were confirmed microscopically to be pheochromocytomas (r = right and l = left).

mas (Fig. 1, right). Extensive necrosis in the left pheochromocytoma was responsible for the relatively less intense accumulation of  $^{11}\text{C}$ -HED in that tumor. The patient became normotensive postoperatively and receives maintenance doses of cortisol and fludrocortisone.

All known lesions within the field of view of the PET camera (i.e., those seen by MIBG scanning) were visualized. Tumor-to-background ratios for  $^{11}\text{C}$ -HED and MIBG studies are presented in Figure 2. Specific accumulation of  $^{11}\text{C}$ -HED by the pheochromocytomas was greater than that of either  $^{131}\text{I}$ - or  $^{123}\text{I}$ MIBG on both planar and tomographic images. Those adrenal glands not harboring pheochromocytoma did not accumulate sufficient  $^{11}\text{C}$ -HED for visualization.

Compared to  $^{131}\text{I}$ MIBG scintigraphy, PET scanning with  $^{11}\text{C}$ -HED detected more lesions with higher contrast. This is illustrated in the study of Patient 2, a 49-yr-old man with a 10-yr history of pheochromocytoma. In 1980, an  $8 \times 10$  cm tumor of the left adrenal was resected. In 1981, metastases to the cervical spine developed and the patient has suffered progressive bony metastatic disease. A  $^{11}\text{C}$ -HED PET scan of the chest acquired 10 min following injection, in comparison with the most revealing images made from  $^{131}\text{I}$ MIBG (at 72 hr), is shown in Figure 3. Discrete lesions within both ribs and vertebral bodies are clearly evident on the HED scan; these foci are difficult to discern on the  $^{131}\text{I}$ MIBG study, and their location in the planar images is unclear. Thus, the resolution offered by PET imaging for  $^{11}\text{C}$ -HED concentrations for the identification of discrete foci of pheochromocytoma is superior to that of the standard  $^{131}\text{I}$ MIBG scintigraphy.

Image quality of the PET examinations also surpassed that obtained with  $^{123}\text{I}$ MIBG SPECT, as demonstrated by the studies of Patient 6. This 42-yr-old man developed hypertension and palpitations in 1978 and a pheochromocytoma of the left adrenal gland was removed. In 1979, symptoms returned and metastatic disease within the ab-

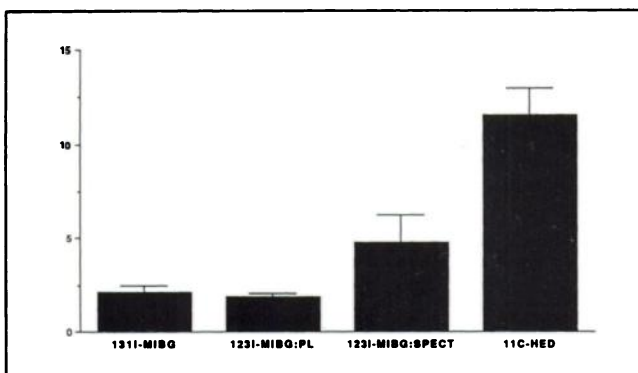


**FIGURE 2.** Tumor-to-background ratios for  $^{131}\text{I}$ MIBG,  $^{123}\text{I}$ MIBG planar and SPECT, and  $^{11}\text{C}$ -HED (mean  $\pm$  s.e.m.). This includes those tumors that could be identified on both MIBG and HED examinations. This index of uptake was greater for  $^{11}\text{C}$ -HED than for  $^{131}\text{I}$ MIBG ( $n = 6$ , paired  $t$ -test,  $p = 0.016$ ),  $^{123}\text{I}$ MIBG planar studies ( $n = 8$ ,  $p = 0.0036$ ) and  $^{123}\text{I}$ MIBG SPECT ( $n = 8$ ,  $p = 0.0002$ ).

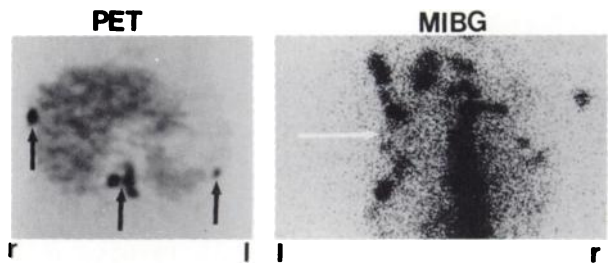


**FIGURE 3.** Patient 2. (Left) HED PET scan of the lower chest-upper abdomen acquired 10 min after injection. The location of this transverse plane is indicated by the light arrow on the MIBG image. Multiple discrete foci are noted in the ribs and vertebrae (arrows). (Right) Posterior image of the chest obtained 72 hr following  $^{131}\text{I}$ MIBG. There is diffusely increased activity in the ribs and spine, but individual lesions cannot be discerned (r = right and l = left).

domen was found. A left para-aortic mass was partially resected in 1980 and subsequently treated with large doses of  $^{131}\text{I}$ MIBG. In 1990, the patient returned for evaluation. Figure 4 compares the  $^{11}\text{C}$ -HED PET study, the  $^{123}\text{I}$ MIBG SPECT examination, and the CT scan. The PET images, obtained only 10 min following injection, clearly delineate the left para-aortic tumor. The intensity of uptake is depicted on the color scale (blue; least intense, white; most intense) and, in comparison to the liver background, is substantially higher than that seen with  $^{123}\text{I}$ MIBG SPECT at 24 hr. The functional representation of the tumor, kidneys and liver seen with the PET scan correspond well to the anatomic definition provided by the CT scan.

The uptake of  $^{11}\text{C}$ -HED into tumors was rapid. Most pheochromocytomas were readily evident within 2 min of administration and all that were detected were seen within 5 min. The time-activity graph for the pheochromocytomas of Patients 1–6 and 8–10 is shown in Figure 5. Accumulation of  $^{11}\text{C}$ -HED occurred promptly after injection. By 5 min, 76% of the uptake at 20 min had occurred and the mean tumor-to-background ratio exceeded 9. Although uptake into the tumors appeared to plateau by 20 min, the tumor-to-nontumor ratios continued to rise due to clearance of radiotracer from the surrounding tissues. For comparison, the much slower accumulation of  $^{123}\text{I}$ MIBG is also shown in Figure 5. The tumor-to-nontumor ratios achieved with  $^{11}\text{C}$ -HED 2 min following injection were similar to those found 24 hr following  $^{123}\text{I}$ MIBG administration.

In patients with metastatic disease, all but one of the lesions visualized by CT scanning within the field of view of the PET camera were detected. In Patient 4, there was a single lung nodule 3 mm diameter, not clearly identifiable in the PET images, and presumed to represent pheochromocytoma. However, in the upper abdomen of the same patient, PET detected three abnormal foci in areas of prior surgery that could not be found by CT.

The pattern of  $^{11}\text{C}$ -HED accumulation by other organs

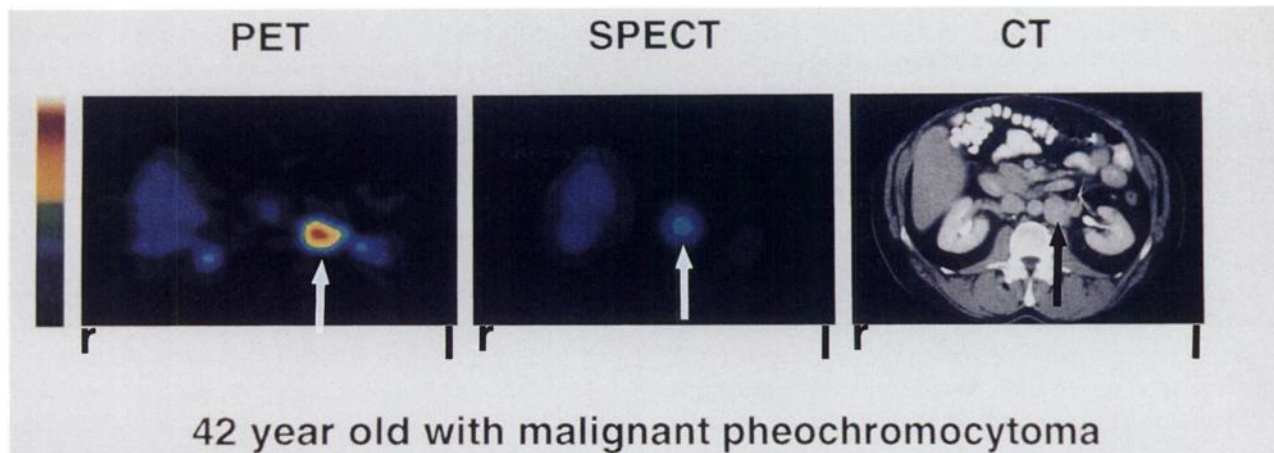


**FIGURE 4.** Patient 6. (Left)  $^{11}\text{C}$ -HED PET scan of the mid-abdomen acquired 10 min after administration. The pheochromocytoma (arrow) is evident anterior and medial to the left kidney. The intensity of uptake is reflected by the color bar (blue; least intense, white; most intense). Activity within the renal collecting systems represents urinary excretion. (Center) Transverse reconstruction of SPECT examination acquired 24 hr after [ $^{123}\text{I}$ ]MIBG at the same level as the PET study. The accumulation of tracer within the tumor, compared to the liver and background activity, is less than that seen on the PET examination. (Right) CT scan shows the left para-aortic mass (arrow). Note that the shape of the tumor and its location in relation to the kidneys and liver are depicted quite well by the PET study (r = right and l = left).

within the field of view of the PET camera differs from that of pheochromocytomas. Figure 6 shows the time-activity curves for the liver, kidney and tumor of Patient 7. There was prompt uptake into the liver but little change in activity after 3 min. Renal accumulation was also rapid. However, activity within the kidneys quickly declined after 4 min due to excretion into the urinary tracts. Tumor uptake of  $^{11}\text{C}$ -HED could be clearly distinguished from nearby liver (Figs. 1 and 3) and kidney (Fig. 4). The tumor of a single patient (#7) failed to accumulate either MIBG or HED.

The uptake of  $^{11}\text{C}$ -HED into pheochromocytomas was unrelated to plasma catecholamine values at the time of

administration ( $p = 0.36$  norepinephrine,  $p = 0.15$  epinephrine). All patients tolerated the investigations well. No side effects were observed and no changes in blood pressure (mean 132/77 mm Hg) or plasma catecholamine levels (Table 1) were found following administration of  $^{11}\text{C}$ -HED.

## DISCUSSION

Carbon-11-HED is the first available positron-emitting probe of the sympathetic nervous system suitable for administration in man. Biodistribution studies in experimental animals showed that this compound accumulates in

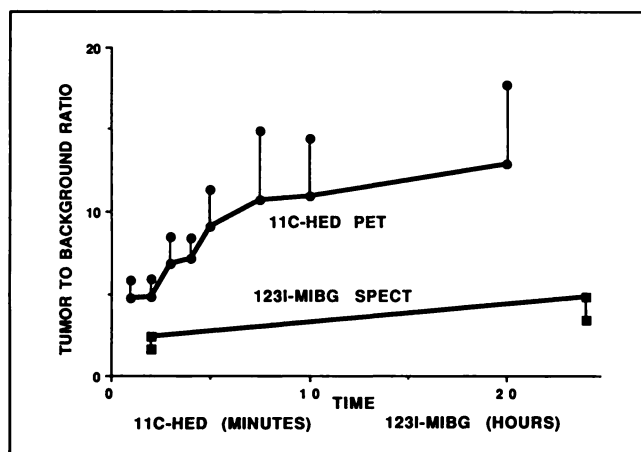


**FIGURE 5.** Tumor-to-background ratios as a function of time (mean  $\pm$  s.e.m.). The x-axis value is minutes following injection of HED (Patients 1–6, 8–10) and hours following injection of [ $^{123}\text{I}$ ]MIBG (Patients 2, 4, 6–10). Most of the uptake of HED occurs quite soon after injection. By 5 min, the tumor-to-nontumor ratio exceeded 9 and the tumors were readily visible. In contrast, the uptake of MIBG was much slower and less than that of HED.

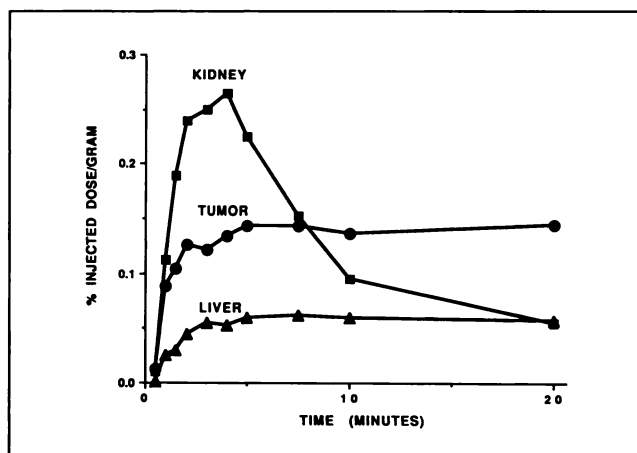


**FIGURE 6.** Time-activity curves of the liver, kidney and pheochromocytoma of Patient 6 (decay-corrected). There is rapid uptake of  $^{11}\text{C}$ -HED by all three tissues. However, the kidney activity declines quickly after 4 min, due to excretion of the tracer into the urine, and falls well below that of the tumor by 10 min. The liver and tumor activity remain nearly constant after 7.5 min. The tumor activity is approximately three-fold that of the liver, and the pheochromocytoma is readily distinguishable.

organs with rich sympathetic innervation, especially the heart and adrenal medulla (13,14). Studies in patients with cardiac transplants, whose hearts are thus denervated, provided further evidence that this tracer is a marker of sympathetic neuronal integrity (14). These findings made it probable that the combination of the favorable chemistry of  $^{11}\text{C}$ -HED and the advanced imaging technology of PET would provide a rapid, sensitive and anatomically precise method to localize deposits of pheochromocytoma.

Carbon-11-HED promptly accumulates in pheochromocytomas, both primary and metastatic deposits, within 5 min of tracer administration. In comparison, imaging with [ $^{123}\text{I}$ ]MIBG, the best available single-photon emitting radiotracer of adrenergic nervous tissue, requires at least 24 hr to achieve optimal tumor-to-background ratios. HED is more polar than MIBG, and there is much less nonspecific uptake. Since specific binding is much greater than nonspecific uptake, tumor-to-background accumulation of HED is quite high very early after injection and pheochromocytomas are visualized within minutes. MIBG requires a relatively lengthy interval for nonspecific accumulation to decline before tumors become identifiable in the large reservoir of background activity.

Pheochromocytomas were demonstrated in 9 of 10 patients. The tumor which failed to accumulate either MIBG or HED secreted dopamine and little norepinephrine and epinephrine. The excised specimen was analyzed in vitro and was found to contain large quantities of dopamine, but very little norepinephrine and epinephrine. Thus, the expected transport and storage mechanisms for norepinephrine appear nonfunctioning. Other tracers, e.g., flourodopa, which are markers for catecholamine synthesis rather than uptake and storage, might be useful to characterize the uncommon tumors which do not concentrate HED. The uptake of HED by pheochromocytomas reflects both catecholamine transport and storage capacity, but the relationship to the rate of secretion of catecholamines is not direct. Relatively high concentrations of HED were found in the tumors of subjects with high (e.g., Patient 4) or normal (e.g., Patient 3) plasma-catecholamine levels.

PET with  $^{11}\text{C}$ -HED is an approach to the investigation of pheochromocytoma that utilizes state-of-the-art imaging technology and a newly developed radiotracer probe of sympathetic neuronal activity. There are several potential advantages of this approach to conventional scintigraphy with MIBG.

1. Tomographic images with high spatial and temporal resolution allow the rapid and confident identification of deposits of pheochromocytoma. Lesions are evident within minutes of injection of  $^{11}\text{C}$ -HED. In contrast, [ $^{131}\text{I}$ ]MIBG scintigraphy may require several days for optimal tumor-to-background characteristics, with some pheochromocytomas not appearing until a week following [ $^{131}\text{I}$ ]MIBG injection (16). Although [ $^{123}\text{I}$ ]MIBG is the best single-photon emitting agent available to image the sympathetic nervous

system and related tumors, imaging still must take place over 2–3 days, multiple patient visits are required and the relatively long half-life limits the dose that can be administered. It is possible that advanced SPECT instrumentation with multiheaded systems may somewhat improve the quality of [ $^{123}\text{I}$ ]MIBG images, but this technology is also expensive and not widely available.

2. The use of a tracer labeled with a short-lived, positron-emitting radionuclide permits the administration of much larger tracer doses with no additional radiation exposure. The radiation dose to the whole body from 20 mCi  $^{11}\text{C}$ -HED is 0.186 rad, less than that from 0.5 mCi [ $^{131}\text{I}$ ]MIBG (0.45 rad) or 10 mCi [ $^{123}\text{I}$ ]MIBG (0.53 rad). Thus, for lower radiation exposure, higher quality images with greater information density are obtained.
3. Because of the short half-life of the  $^{11}\text{C}$  radiolabel (20 min), the residual activity within the patient at the conclusion of the study is very low, obviating concerns of exposure to nursing staff and families to incidental radiation. There is minimal radioactive waste material to be discarded. This may become especially important in the management of young patients with another adrenergic tumor, neuroblastoma, for whom the disposal of diapers contaminated with long-lived radioisotopes poses logistical concerns that are simplified by the use of a shorter-lived agent.
4. The PET technique allows more precise quantitation of uptake, which may be useful in following the effect of therapeutic regimens on tumor behavior and the calculation of radiation doses.
5. Tracer kinetic modeling may provide a quantitative measure of catecholamine uptake and storage. This might then be used to identify tumors with high norepinephrine content and thus patients at highest risk for hypertensive crises.
6. Along with  $^{11}\text{C}$ -HED, other short-lived tracers can be used to examine certain biologic features, including blood flow, oxygen and glucose metabolism and amino acid incorporation in a single setting. These determinations could be particularly helpful in assessing the response to therapy of tumors such as malignant pheochromocytoma and neuroblastoma, which frequently require systemic treatment.

There are, however, potential disadvantages to this technique. Currently, the costs of the study are high and the availability limited. Carbon-11-HED is the first positron-emitting tracer of the sympathetic nervous system suitable for administration in man. The synthesis is relatively complex and the short half-life of  $^{11}\text{C}$  requires onsite production for each patient. Other compounds labeled with  $^{18}\text{F}$  (half-life 110 min) under development, such as fluorodopamine, fluoronorepinephrine and fluorometaraminol, may be preferable for delivery to outlying PET

centers from regional cyclotron-chemistry units (17,18). In addition, PET is not yet ideally suited to screening the entire body. However, PET cameras may be operated in rectilinear mode and whole-body information may be displayed as a series of longitudinal images (19).

In summary, we have shown that PET imaging with <sup>11</sup>C-HED is a promising approach to the detection and localization of pheochromocytoma. Further studies are required to determine the efficacy of this technique and its utility in the imaging of other neuroendocrine tumors.

#### ACKNOWLEDGMENTS

Special thanks to Shirley Mallette, RN and Elizabeth Mudgett, RN for assistance in patient care, to Christine Allman, CNMT, Annette Betley, CNMT, Leslie Botti, CNMT, Vince McCormick, CNMT, Edward McKenna, CNMT, Jill Rothley, CNMT and Andrew Weeden, CNMT, for technological expertise and support, to the cyclotron staff for the preparation of <sup>11</sup>C, to Ngoc Nguyen for aid in graphical design, to Joyce Stafford for typing the manuscript, and to William H. Beierwaltes, MD, without whose long-standing interest in pheochromocytoma, this work would not have been possible.

This work was presented in part at the European Association of Nuclear Medicine Congress, 1990, Amsterdam, The Netherlands and at the 37th Annual Meeting of the Society of Nuclear Medicine, 1990, Washington, D.C.

This work was supported by FIRST Award 1 R29 CA54216 01 from the National Cancer Institute (BLS) and by a grant (#MO1RR00042) from the Clinical Research Center of the University of Michigan.

#### REFERENCES

1. Samaan NA, Hickey RC, Shutts PE. Diagnosis, localization, and management of pheochromocytoma. *Cancer* 1988;62:2451-2469.
2. Bravo EL. Clinical aspects of endocrine hypertension. *Med Clin N Am* 1987;71:907-920.
3. Krane NK. Clinically unsuspected pheochromocytomas. Experience at Henry Ford Hospital and a review of the literature. *Arch Intern Med* 1986;146:54-57.
4. Welch TJ, Sheedy PF, van Heerden JA, Sheps SF, Hattery RR, Stephens DH. Pheochromocytoma: value of computed tomography. *Radiology* 1983;141:211-218.
5. Francis IR, Glazer GM, Shapiro B, Sisson JC, Gross BH. Complementary roles of CT and <sup>131</sup>I-MIBG scintigraphy in diagnosing pheochromocytoma. *AJR* 1983;141:710-725.
6. Quint LE, Glazer GM, Francis IR, Shapiro B, Chenevert TL. Pheochromocytoma and paraganglioma: comparison of MR imaging with CT and I-131 MIBG scintigraphy. *Radiology* 1987;165:89-93.
7. Wieland DM, Wu JL, Brown LE, Mangner TJ, Swanson DP, Beierwaltes WH. Radiolabeled adrenergic neuron blocking agents: adrenomedullary imaging with <sup>131</sup>I-iodobenzylguanidine. *J Nucl Med* 1980;21:349-353.
8. Sisson JC, Frager MS, Valk TW, et al. Scintigraphic localization of pheochromocytoma. *N Engl J Med* 1981;305:12-17.
9. Shapiro B, Copp JE, Sisson JC, Eyre PL, Wallis J, Beierwaltes WH. Iodine-131-meta-iodobenzylguanidine for the locating of suspected pheochromocytoma: experience in 400 cases. *J Nucl Med* 1985;26:576-585.
10. Velchik MG, Alavi A, Kressel HY, Engelman K. Localization of pheochromocytoma: MIBG, CT, and MRI correlation. *J Nucl Med* 1989;30:328-336.
11. Chatal JF, Charbonnel B. Comparison of iodobenzylguanidine imaging with computed tomography in locating pheochromocytoma. *J Clin Endocrinol Metab* 1985;61:769-772.
12. Lynn MD, Shapiro B, Sisson JC, et al. Pheochromocytomas and the normal adrenal medulla: improved visualization with <sup>123</sup>I-MIBG scintigraphy. *Radiology* 1985;156:789-792.
13. Rosenspire KC, Haka MS, Jewett DM, et al. Synthesis and preliminary evaluation of [<sup>11</sup>C]methoxyephedrine: a false neurotransmitter agent for heart neuronal imaging. *J Nucl Med* 1990;31:1328-1334.
14. Schwaiger M, Kalff V, Rosenspire KC, et al. The noninvasive evaluation of the sympathetic nervous system in the human heart by PET. *Circulation* 1990;82:457-464.
15. Khafagi FA, Shapiro B, Fig LM, Mallette S, Sisson JC. Labetalol reduces iodine-131-MIBG uptake by pheochromocytoma and normal tissues. *J Nucl Med* 1989;30:481-489.
16. Lindberg S, Fjalling M, Jacobsson, Jansson, Tisell L-E. Methodology and dosimetry in adrenal medullary imaging with iodine-131-MIBG. *J Nucl Med* 1988;29:1638-1643.
17. Eisenhofer G, Hovey-Sion D, Kopin IJ, et al. Neuronal uptake and metabolism of 2- and 6-fluorodopamine: false neurotransmitters for positron emission tomographic imaging of sympathetically innervated tissues. *J Pharmacol Exp Ther* 1989;225:419-427.
18. Schwaiger M, Guiborg H, Rosenspire K, et al. Effect of regional myocardial ischemia on sympathetic nervous system as assessed by fluorine-18-metaraminol. *J Nucl Med* 1990;31:1352-1357.
19. Schiepers C, Hawkins RA, Hoh C, et al. Total-body imaging with fluorodeoxyglucose (FDG) and PET in patients with malignancies. *J Nucl Med* 1990;31:803.